

The following resources related to this article are available online at www.sciencemag.org (this information is current as of November 24, 2009):

Updated information and services, including high-resolution figures, can be found in the online version of this article at:

<http://www.sciencemag.org/cgi/content/full/307/5707/258>

Supporting Online Material can be found at:

<http://www.sciencemag.org/cgi/content/full/307/5707/258/DC1>

A list of selected additional articles on the Science Web sites **related to this article** can be found at:

<http://www.sciencemag.org/cgi/content/full/307/5707/258#related-content>

This article **cites 17 articles**, 10 of which can be accessed for free:

<http://www.sciencemag.org/cgi/content/full/307/5707/258#otherarticles>

This article has been **cited by** 34 article(s) on the ISI Web of Science.

This article has been **cited by** 9 articles hosted by HighWire Press; see:

<http://www.sciencemag.org/cgi/content/full/307/5707/258#otherarticles>

This article appears in the following **subject collections**:

Medicine, Diseases

<http://www.sciencemag.org/cgi/collection/medicine>

Information about obtaining **reprints** of this article or about obtaining **permission to reproduce this article** in whole or in part can be found at:

<http://www.sciencemag.org/about/permissions.dtl>

of the uptake of *S. typhimurium* by DCs within the intestinal mucosa. Most likely as a consequence of impaired bacterial sampling by DCs, *cx₃cr1^{GFP/GFP}* mice displayed enhanced susceptibility to *S. typhimurium* infection. Thus, they succumbed within 6 days of oral administration of 1×10^9 bacteria and displayed significantly higher bacterial loads in their organs, compared with the relative resistance of their *cx₃cr1^{GFP/+}* and wild-type counterparts (Fig. 4, C and D). Delayed pathogen uptake by DCs from the lumen and the lamina propria may thus form the mechanistic foundation for the impaired antibacterial defense in CX₃CR1-deficient mice.

We have demonstrated an extensive intestinal DC network that serves as a gateway for the uptake and transport of the intestinal microbiota. We have identified and characterized CX₃CR1-positive lamina propria DCs, a major component of this system, which are capable of taking up bacteria by way of transepithelial dendrites in order to provide defense against pathogenic microorganisms. CX₃CR1 deficiency results in a defect of lamina propria DCs that impairs the sampling of bacteria from the intestinal lumen and impedes their ability to take up invasive pathogens *in vitro*. The intrinsic functional programs and subspecifications of CX₃CR1-positive and -negative DCs in mucosal innate and adaptive immune responses will need to be further defined. Nevertheless, CX₃CR1-dependent regulation of DCs appears to provide a central mechanism for the control of the mucosal defense against entero-invasive bacteria.

The interaction of DCs with the intestinal microbiota by the way of CX₃CR1-dependent transepithelial dendrites could activate an innate immune pathway that protects the mucosa from pathogenic bacteria. The formation of these dendrites may be linked to the immature phenotype of lamina propria DCs and associated with their phagocytic function. Their use thus constitutes a mechanism by which DCs could take up intestinal antigens, which is distinct from previously established systems involving M cells. We propose that the CX₃CR1-dependent and the M cell-dependent systems could thus be associated with specific DC subsets. It will be important to determine whether such networks operate synergistically as redundant systems or if they have distinct functions in the recognition of commensal and pathogenic bacteria. Luminal sampling by CX₃CR1-positive DCs occurs by globular structures formed at the end of transepithelial dendrites, which could serve as luminal sensors for the mucosal immune system to continually monitor intestinal content. Characterization of the surface components that facilitate antigen uptake through this spe-

cialized cellular compartment may aid in developing strategies to prevent bacterial and viral pathogens from co-opting this route during infection. Furthermore, targeting of antigens to transepithelial dendrites could be used to directly engage the function of intestinal CX₃CR1-positive DCs in vaccine development.

References and Notes

1. H. H. Uhlig, F. Powrie, *J. Clin. Invest.* **112**, 648 (2003).
2. B. L. Kelsall, C. A. Biron, O. Sharma, P. M. Kaye, *Nature Immunol.* **3**, 699 (2002).
3. M. R. Neutra, A. Frey, J. P. Kraehenbuhl, *Cell* **86**, 345 (1996).
4. I. Mellman, R. M. Steinman, *Cell* **106**, 255 (2001).
5. J. Banchereau *et al.*, *Ann. N.Y. Acad. Sci.* **987**, 180 (2003).
6. A. Iwasaki, B. L. Kelsall, *J. Exp. Med.* **190**, 229 (1999).
7. M. H. Jang *et al.*, *Proc. Natl. Acad. Sci. U.S.A.* **101**, 6110 (2004).
8. F. P. Huang, C. F. Farquhar, N. A. Mabbott, M. E. Bruce, G. G. MacPherson, *J. Gen. Virol.* **83**, 267 (2002).
9. A. J. Macpherson, T. Uhr, *Science* **303**, 1662 (2004).
10. I. Maric, P. G. Holt, M. H. Perdue, J. Bienenstock, *J. Immunol.* **156**, 1408 (1996).
11. M. Rescigno *et al.*, *Nature Immunol.* **2**, 361 (2001).

12. Materials and methods are available as supporting material on Science Online.
13. S. Jung *et al.*, *Mol. Cell. Biol.* **20**, 4106 (2000).
14. A. Muehlhoefer *et al.*, *J. Immunol.* **164**, 3368 (2000).
15. A. D. Lucas *et al.*, *Am. J. Pathol.* **158**, 855 (2001).
16. F. Geissmann, S. Jung, D. R. Littman, *Immunity* **19**, 71 (2003).
17. J. H. Niess *et al.*, data not shown.
18. A. Iwasaki, B. L. Kelsall, *J. Exp. Med.* **191**, 1381 (2000).
19. D. N. Cook *et al.*, *Immunity* **12**, 495 (2000).
20. X. Zhao *et al.*, *J. Immunol.* **171**, 2797 (2003).
21. Supported by grants DK54427, DK43351, and DK33506 (H.C.R.) and AI33856 (D.R.L.). J.H.N. was supported by the Deutsche Forschungsgemeinschaft (NI575/2-1) and a Research Fellowship Award from the Crohn's and Colitis Foundation of America. D.R.L. is an investigator of the Howard Hughes Medical Institute. S.J. is an incumbent of the Pauline Recanati Career Development Chair and Scholar of the Benozio Center for Molecular Medicine.

Supporting Online Material

www.sciencemag.org/cgi/content/full/307/5707/254/DC1

Materials and Methods

Figs. S1 and S2

References

Movies S1 to S4

19 July 2004; accepted 15 November 2004
10.1126/science.1102901

Anticonvulsant Medications Extend Worm Life-Span

Kimberley Evason, Cheng Huang, Idella Yamben, Douglas F. Covey, Kerry Kornfeld*

Genetic studies have elucidated mechanisms that regulate aging, but there has been little progress in identifying drugs that delay aging. Here, we report that ethosuximide, trimethadione, and 3,3-diethyl-2-pyrrolidinone increase mean and maximum life-span of *Caenorhabditis elegans* and delay age-related declines of physiological processes, indicating that these compounds retard the aging process. These compounds, two of which are approved for human use, are anticonvulsants that modulate neural activity. These compounds also regulated neuromuscular activity in nematodes. These findings suggest that the life-span-extending activity of these compounds is related to the anticonvulsant activity and implicate neural activity in the regulation of aging.

Aging is characterized by widespread degenerative changes. Although treatments for aging would be desirable, the development of such treatments is challenging. Approaches based on rational design require information about the aging process, but little information is currently available. Approaches based on random screens of potential treatments require relevant and feasible assays of aging, but the time and effort necessary to measure aging are substantial obstacles.

To address these challenges, we exploited the *C. elegans* model system. These animals age rapidly, and many processes are conserved between nematodes and vertebrates,

including aspects of the aging process (1). To identify compounds that delay aging, we assayed 19 drugs from a variety of functional or structural classes that have known effects on human physiology (2). We reasoned that such compounds might have an undiscovered effect on aging. For each drug, hermaphrodites were cultured with three different concentrations from before fertilization until death, and the adult life-span [fourth larval (L4) stage to death] of about 50 animals was measured. To focus on aging, we excluded dead worms that displayed internally hatched progeny, an extruded gonad, or desiccation due to crawling off the agar.

Ethosuximide had the greatest effect on adult life-span, extending mean adult life-span from 16.7 to 19.6 days (17% increase) (Fig. 1B and Table 1). A dose-response analysis revealed that worms cultured with external concentrations of 2 and 4 mg/ml ethosuxi-

Department of Molecular Biology and Pharmacology, Washington University School of Medicine, St. Louis, MO 63110, USA.

*To whom correspondence should be addressed.
E-mail: kornfeld@molecool.wustl.edu

mide displayed the largest extensions of mean life-span; lower concentrations caused smaller extensions, whereas higher concentrations caused toxicity and reduced life-span (3). This effect was temperature sensitive; ethosuximide extended mean life-span by 35% at 15°C, 17% at 20°C, and insignificantly at 25°C (3).

Ethosuximide is a small heterocyclic ring compound that prevents absence seizures in humans and has been a preferred drug for treating this disorder since its introduction in the 1950s (4, 5) (Fig. 1A). An important question is whether the anticonvulsant activity in humans and the life-span extension activity in worms have a similar mechanism. If this is the case, then other drugs with similar structures and anticonvulsant activity might also affect life-span. Trimethadione and 3,3-diethyl-2-pyrrolidinone (DEABL) have anticonvulsant activity and structures

similar to that of ethosuximide (4, 6) (Fig. 1A). Trimethadione is approved for human use and the treatment of absence seizures. DEABL is not used to treat humans. Both compounds caused significant extensions of mean and maximum life-span (Fig. 1, C and D, and Table 1). Trimethadione caused the largest extension of mean (47%) and maximum (57%) life-span of the three compounds. Succinimide, similar in structure but lacking in anticonvulsant activity in vertebrates, did not extend life-span (Fig. 1A and Table 1). These findings suggest that ethosuximide, trimethadione, and DEABL may extend life-span by a similar mechanism that may be related to the mechanism of anticonvulsant activity.

For the treatment of seizures, the therapeutic range of ethosuximide in humans is 40 to 100 µg/ml (5). Worms cultured with an external concentration of 2 mg/ml ethosuxi-

mide had an internal concentration (±SD) of 30.5 ± 22.2 µg/ml. This value is near the therapeutic range, suggesting that the anticonvulsants may have similar targets in worms and humans.

To determine the developmental stage at which the drugs function to extend life-span, trimethadione was administered from fertilization until the L4 stage or from the L4 stage until death. Exposure to trimethadione only during embryonic and larval development had no effect on life-span. In contrast, exposure to trimethadione only during adulthood caused a significant extension of mean life-span (24%) (Fig. 1D and Table 1).

To determine whether these drugs delay age-related declines of physiological processes, we analyzed self-fertile reproduction, body movement, and pharyngeal pumping. The declines of pharyngeal pumping and body movement are positively correlated with each

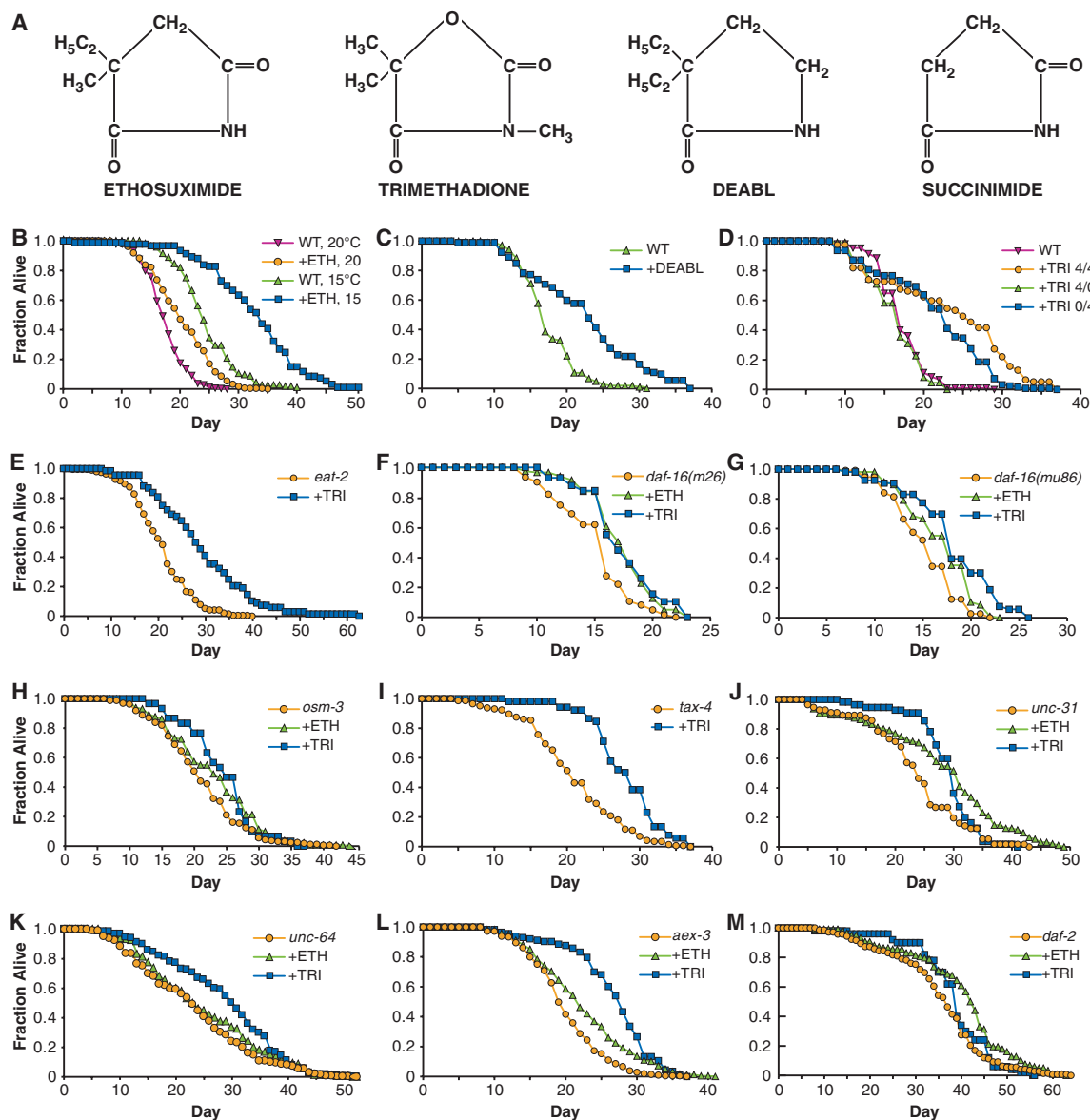


Fig. 1. Anticonvulsants extend adult worm life-span. (A) Compounds. (B to M) Hermaphrodite survival of [(B) to (D)] wild type (WT), (E) *eat-2(ad465)*, (F) *daf-16(m26)* (G) *daf-16(mu86)*, (H) *osm-3(p802)*, (I) *tax-4(p678)*, (J) *unc-31(e928)*, (K) *unc-64(e246)*, (L) *aex-3(ad418)*, and (M) *daf-2(e1370)*. Worms were exposed to ethosuximide (+ETH), DEABL (+DEABL), trimethadione from fertilization until L4 (+TRI 4/0), trimethadione from L4 until death (+TRI 0/4), or trimethadione until death (+TRI 4/4 and +TRI). Dosages are shown in Table 1.

other and with life-span (7). The decline of self-fertile reproduction is not correlated with life-span, suggesting that this age-related change is regulated independently (7). Treatments with ethosuximide and/or trimethadione significantly extended the span of time that animals displayed fast body movement, fast pharyngeal pumping, and any pharyngeal pumping (Fig. 2, B to D and F). Neither compound significantly extended the span of time that animals displayed self-fertile reproduction (Fig. 2, A and F). These measurements can be used to define stages of aging (7). Both compounds extended Stage II, the postreproductive period characterized by vigorous activity (Fig. 2E). Trimethadione also extended Stage IV, the terminal phase characterized by minimal activity. These findings indicate that ethosuximide and trimethadione delay the aging process.

Several genetic and environmental manipulations can extend *C. elegans* life-span. To investigate the relationships between the anticonvulsants and these regulators of aging, we examined the effect of combining two treatments. Worms cultured on nonpathogenic *Bacillus subtilis* or ultraviolet (UV)-irradiated *E. coli* display an extended life-span (8, 9). Trimethadione extended the life-span of worms cultured on *B. subtilis* and UV-irradiated *E. coli* (Table 1), indicating that the primary mechanism of the anticonvulsant life-span extension is not a reduction of bacterial pathogenicity.

Nutrient limitation extends life-span and can be caused by a mutation of the *eat-2* gene that is important for pharyngeal pumping (1, 10, 11). Trimethadione significantly extended the life-span of *eat-2* mutants (42%) (Fig. 1E and Table 1), indicating that the primary mechanism of life-span extension is not nutrient limitation. Furthermore, wild-type animals treated with ethosuximide or trimethadione were not nutrient limited, because they displayed normal pharyngeal pumping, food ingestion, and body morphology (they did not appear thin or starved), and they produced an approximately normal number of progeny (3).

An insulin-like signaling pathway regulates *C. elegans* life-span. This pathway requires the function of sensory neurons that may mediate the release of an insulin-like ligand, the *daf-2* insulin-like growth factor (IGF) receptor gene, and a signal transduction cascade that regulates the *daf-16* forkhead transcription factor gene. Loss-of-function *daf-16* mutations reduce life-span and suppress the life-span extensions caused by mutations in upstream signaling pathway genes such as *daf-2* (12). Treatment with ethosuximide or trimethadione significantly extended the life-span of two loss-of-function mutants, *daf-16(m26)* (16%) and *daf-16(mu86)* (11 to 21%) (Fig. 1, F and G, and

Table 1), although the percentage change caused by trimethadione was less than that in wild-type animals (47%). These results indicate that part of the anticonvulsant action is independent of *daf-16*. Part of the anticonvulsant action may require *daf-16*. However, the reduced effect of trimethadione is consistent with other possibilities, such as deleterious consequences of combining a mutation and a drug that both cause pleiotropic effects (13).

Life-span extension is caused by loss-of-function mutations of genes important

for the function of sensory neurons (*osm-3* and *tax-4*), for neurotransmission (*unc-31*, *unc-64*, and *aex-3*), and for transmission of the insulin-like signal (*daf-2*) (12, 14, 15) (Table 1). Ethosuximide and/or trimethadione significantly increased the life-span of *osm-3*, *tax-4*, *unc-31*, *unc-64*, *aex-3*, and *daf-2* loss-of-function mutants from 8 to 36% (Fig. 1, H to M, and Table 1). These results indicate that part of the anticonvulsant action may be different than the action of these mutations. The effects of ethosuximide and/or trimethadione were only partially additive with several

Table 1. Mean and maximum life-spans. Most strains were fed live *E. coli* OP50 and cultured at 20°C. Exceptions were wild-type strain N2 cultured at 15°C (WT, 15°C), N2 fed live *B. subtilis* (WT, *B. subtilis*), and N2 fed UV-killed OP50 (WT, UV/*E. coli*). External drug concentrations are shown in milligrams per milliliter for ethosuximide (ETH), trimethadione (TRI), and succinimide (SUC). (4/0) and (0/4) indicate culture with drug from fertilization to L4 and L4 to death, respectively. Genotypes with no drug treatment are compared with line 1, and differences were not analyzed for statistical significance. Otherwise, comparisons are to the same genotype with no drug treatment. For these comparisons in the columns showing life-spans, numbers with no asterisks are not significant ($P > 0.05$); *, $P < 0.05$; **, $P < 0.005$; ***, $P < 0.0001$. Maximum adult life-span is the mean life-span of the 10% of the population that had the longest life-spans. *N*, number of hermaphrodites analyzed, with number of independent experiments in parentheses. N.D., not determined.

Genotype	Drug	Mean life-span ± SD (days)	% Change in mean life-span	Maximum life-span ± SD (days)	% Change in maximum life-span	<i>N</i>
WT	None	16.7 ± 3.7		23.3 ± 1.7		976(19)
	ETH(2)	18.9 ± 6.0***	+13	28.9 ± 1.7***	+24	479(10)
	ETH(4)	19.6 ± 5.3***	+17	28.5 ± 1.8***	+22	458(10)
	TRI(4)	24.6 ± 8.4***	+47	36.5 ± 2.2***	+57	482(9)
	TRI (0/4)	20.7 ± 6.7***	+24	30.1 ± 2.3***	+29	124(2)
	TRI (4/0)	15.5 ± 3.4	-7	21.0 ± 1.0	-10	110(2)
	DEABL(2)	21.8 ± 7.6***	+31	34.7 ± 1.6***	+49	92(2)
	SUC(2)†	16.0 ± 4.0	-4	23.5 ± 1.9	+1	94(2)
	WT, 15°C	None	23.6 ± 5.3	+41	32.9 ± 2.7	+41
ETH(4)		31.9 ± 8.2***	+35	45.2 ± 2.4***	+37	93(2)
WT, <i>B. subtilis</i>	None	19.5 ± 5.4	+17	28.8 ± 1.5	+24	108(2)
	TRI(4)	27.1 ± 6.6***	+39	38.2 ± 1.8***	+33	115(2)
WT, UV/ <i>E. coli</i>	None	20.0 ± 6.3	+20	30.4 ± 2.3	+30	51(2)
	ETH(4)	22.8 ± 4.8*	+14	29.8 ± 1.4	-2	45(2)
	TRI(4)	28.1 ± 6.0***	+41	37.3 ± 0.7**	+23	49(2)
<i>daf-16</i> (m26)	None	14.4 ± 3.3	-14	20.0 ± 1.0	-14	123(3)
	ETH(2)	16.7 ± 3.0***	+16	21.3 ± 0.8**	+7	119(3)
	TRI(2)	16.7 ± 3.2***	+16	22.0 ± 0.0 (N.D.)	+10	58(1)
<i>daf-16</i> (mu86)	None	14.4 ± 3.2	-14	19.6 ± 0.9	-16	113(2)
	ETH (0.5)	16.0 ± 3.5**	+11	21.1 ± 0.5**	+8	105(2)
	TRI(4)	17.4 ± 4.5**	+21	24.2 ± 1.2**	+23	53(1)
<i>daf-2</i> (e1370)	None	34.6 ± 10.9	+107	52.6 ± 5.0	+126	142(3)
	ETH(4)	39.3 ± 11.5**	+14	56.8 ± 2.9*	+8	118(3)
	TRI(4)	37.6 ± 8.5*	+9	50.0 ± 3.5	-5	50(1)
<i>unc-31</i> (e928)	None	22.8 ± 8.4	+37	36.2 ± 3.3	+55	56(3)
	ETH(2)	27.4 ± 11.1**	+20	44.4 ± 2.4***	+23	95(3)
	TRI(4)	28.3 ± 5.4***	+24	35.8 ± 2.4	-1	55(1)
<i>unc-64</i> (e246)	None	22.6 ± 10.7	+35	42.8 ± 3.3	+84	227(4)
	ETH(2)	24.4 ± 10.7*	+8	43.7 ± 2.6*	+2	160(3)
	TRI(4)	28.1 ± 10.2***	+24	43.3 ± 2.9	+1	245(2)
<i>aex-3</i> (ad418)	None	19.3 ± 5.3	+16	29.1 ± 2.5	+25	209(4)
	ETH(4)	21.8 ± 6.8***	+13	34.4 ± 2.1***	+18	236(4)
	TRI(4)	26.0 ± 6.0***	+35	34.3 ± 1.0***	+18	113(2)
<i>tax-4</i> (p678)	None	20.1 ± 6.6	+20	31.4 ± 2.4	+35	144(3)
	TRI(4)	27.4 ± 4.9***	+36	35.2 ± 1.2*	+12	52(1)
<i>osm-3</i> (p802)	None	20.2 ± 6.6	+21	32.1 ± 4.1	+38	161(4)
	ETH(2)	22.1 ± 7.1	+9	34.0 ± 3.6	+6	131(3)
	TRI(4)	23.6 ± 5.4**	+17	32.7 ± 3.0	+2	30(1)
<i>eat-2</i> (ad465)	None	20.1 ± 6.3	+20	31.4 ± 3.1	+35	192(4)
	TRI(4)	28.6 ± 10.0***	+42	47.2 ± 7.3**	+50	68(1)

†Concentrations of 0.5, 5, or 10 mg/ml succinimide also did not significantly increase mean life-span.

mutations, notably *daf-2*, *unc-64*, and *osm-3*. Thus, part of the activity of the anticonvulsants may be similar to the effects of these mutations, several of which affect neural func-

tion. However, an absence of full additivity is also consistent with other possibilities (13).

Anticonvulsants affect the neural activity of vertebrates. To determine whether these

drugs have a similar activity in nematodes, we analyzed neuromuscular behaviors. *C. elegans* egg laying is mediated by HSN neurons that innervate the vulval muscles (16, 17). Wild-type hermaphrodites lay eggs that have matured to about the 30-cell stage of development. Trimethadione and ethosuximide caused wild-type hermaphrodites to lay eggs at much earlier stages of development, often the 1- to 7-cell stage (Fig. 3C). The control drug, succinimide, did not stimulate egg laying (Fig. 3C). A delay in egg laying can result in an egg-laying defective (Egl) phenotype characterized by progeny that hatch internally. Approximately 8.9% of wild-type hermaphrodites displayed an Egl phenotype during their lifetime; ethosuximide and trimethadione reduced this to 2.9 and 1.2%, respectively (Fig. 3A). To investigate whether the anticonvulsants act presynaptically on the HSN neurons or postsynaptically on the vulval muscles, we analyzed an *egl-1* mutant that lacks HSNs as a result of a developmental abnormality (17). Ethosuximide did not cause *egl-1* mutants to lay eggs at earlier stages of development (Fig. 3D), indicating that the vulval muscles are not sufficient and the HSN neurons are necessary for the anticonvulsant to stimulate egg laying. This result is consistent with the model that the drug acts presynaptically.

Treatment with ethosuximide or trimethadione caused wild-type hermaphrodites to display hyperactive motility, indicating that these drugs stimulate neuromuscular activity (Fig. 3B). To analyze this phenotype, we

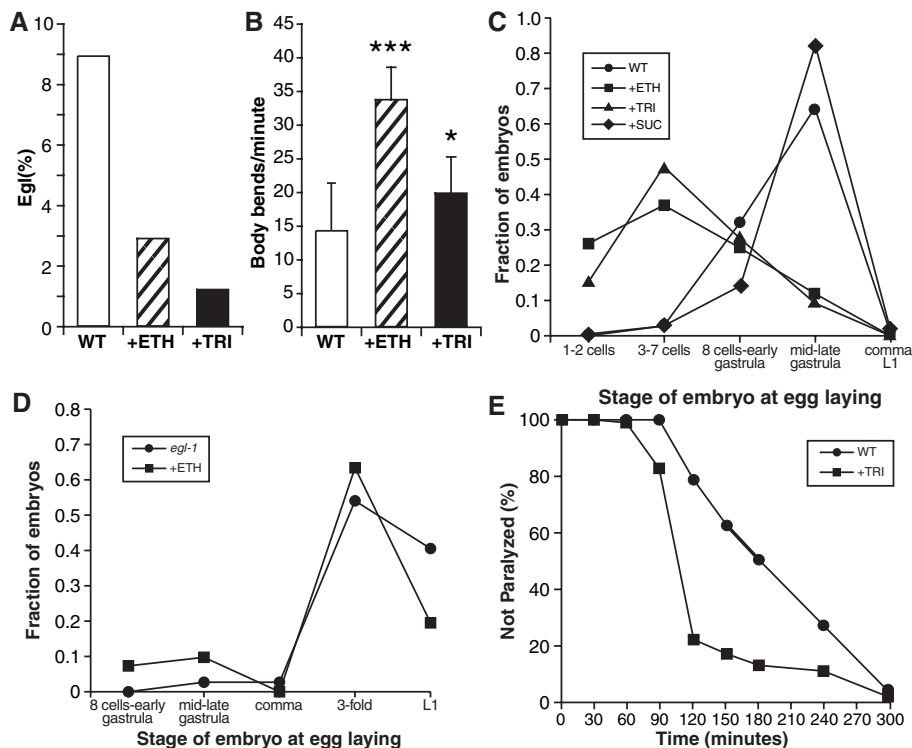
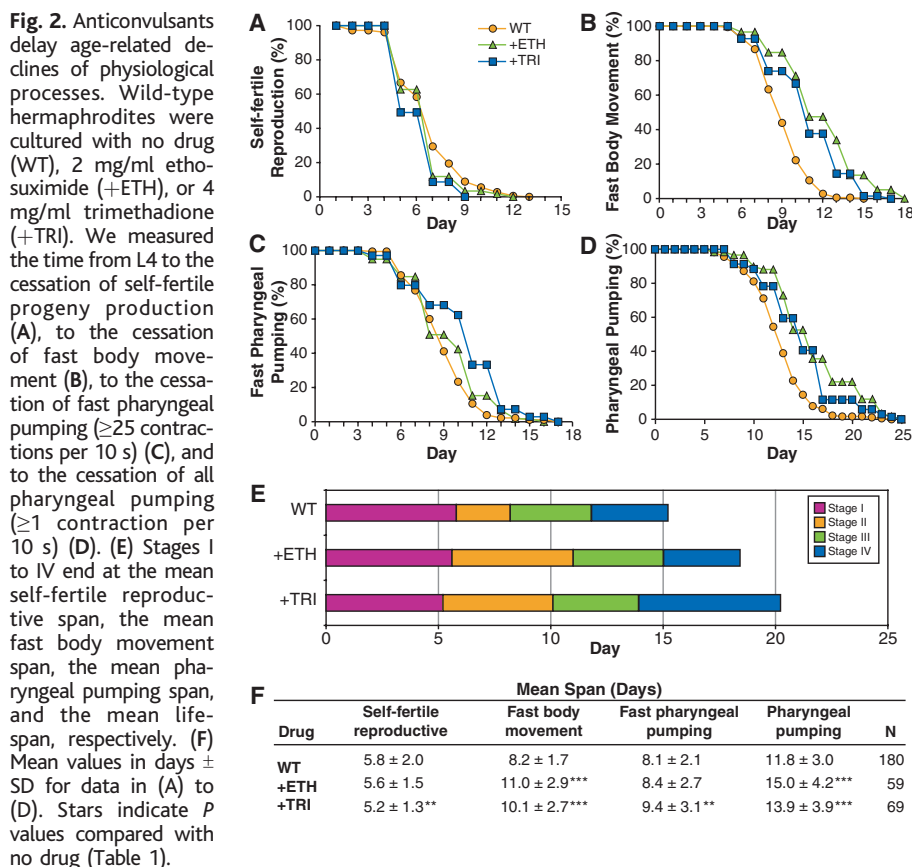


Fig. 3. Anticonvulsants stimulate neuromuscular activity. (A) The percent of dead hermaphrodites that displayed internally hatched progeny (Egl) with no drug (WT), 2 mg/ml ethosuximide (+ETH), or 4 mg/ml trimethadione (+TRI) ($n > 150$). (B) Motility of wild-type young adult hermaphrodites with no drug ($n = 13$), 2 mg/ml ethosuximide ($n = 8$), 4 mg/ml trimethadione ($n = 14$). Stars indicate P values compared to no drug (Table 1). (C and D) The developmental stage of embryos at the time of egg laying. (C) Wild-type young adult hermaphrodites treated with no drug ($n = 107$), 2 mg/ml ethosuximide ($n = 92$), 4 mg/ml trimethadione ($n = 119$), or 2 mg/ml succinimide (+SUC) ($n = 44$). (D) *egl-1*($n487$) young adult hermaphrodites treated with no drug ($n = 37$) or 2 mg/ml ethosuximide ($n = 41$). (E) A time course of paralysis induced by aldicarb in wild-type young adult hermaphrodites treated with no drug ($n = 99$) or 4 mg/ml trimethadione ($n = 99$).

examined sensitivity to the acetylcholinesterase inhibitor aldicarb. Aldicarb causes paralysis of body movement resulting from the accumulation of acetylcholine at the neuromuscular junction (18). Mutations that reduce synaptic transmission cause resistance to aldicarb (18). In contrast, mutations that stimulate synaptic transmission cause hypersensitivity to aldicarb-mediated paralysis (19). Trimethadione treatment of wild-type animals caused hypersensitivity to aldicarb-mediated paralysis (Fig. 3E). The control drug, succinimide, did not cause hyperactive motility or aldicarb hypersensitivity (3). These results indicate the anticonvulsants stimulate synaptic transmission in the neuromuscular system that controls body movement.

Ethosuximide and trimethadione effectively treat absence seizures in humans by regulating neural activity. A likely target of ethosuximide is T-type calcium channels, although it is possible that these compounds act on multiple targets (20–22). These anticonvulsants also affected neural activity in nematodes, and the anticonvulsant and the life-span extension effects of the compounds may act through similar mechanisms. The findings presented here are consistent with the model that the effect on neural activity causes the life-span extension, although they do not exclude the possibility that the drugs affect neural activity and aging by different mechanisms. Furthermore, the interactions with the insulin-signaling mutants suggest the intriguing possibility that neural activity regulates aging by both *daf-16*-dependent and *daf-16*-independent mechanisms.

References and Notes

1. L. Guarente, C. Kenyon, *Nature* **408**, 255 (2000).
2. Materials and methods are available as supporting material on Science Online.
3. S. Hughes, K. Evason, data not shown.
4. B. G. Katzung, Ed., *Basic and Clinical Pharmacology* (Appleton and Lange, Upper Saddle River, NJ, ed. 7, 1998).
5. R. H. Levy, R. H. Mattson, B. S. Meldrum, E. Perucca, Eds., *Antiepileptic drugs* (Lippincott, Williams and Wilkins, Philadelphia, ed. 5, 2002).
6. P. A. Reddy *et al.*, *J. Med. Chem.* **39**, 1898 (1996).
7. C. Huang, C. Xiong, K. Kornfeld, *Proc. Natl. Acad. Sci. U.S.A.* **101**, 8084 (2004).
8. D. Gems, D. L. Riddle, *Genetics* **154**, 1597 (2000).
9. D. A. Garsin *et al.*, *Science* **300**, 1921 (2003).
10. J. P. McKay, D. M. Raizen, A. Gottschalk, W. R. Schafer, L. Avery, *Genetics* **166**, 161 (2004).
11. B. Lakowski, S. Hekimi, *Proc. Natl. Acad. Sci. U.S.A.* **95**, 13091 (1998).
12. C. Kenyon, J. Chang, E. Gensch, A. Rudner, R. Tabtiang, *Nature* **366**, 461 (1993).
13. D. Gems, S. Pletcher, L. Partridge, *Aging Cell* **1**, 1 (2002).
14. J. Apfeld, C. Kenyon, *Nature* **402**, 804 (1999).
15. M. Ailion, T. Inoue, C. I. Weaver, R. W. Holdcraft, J. H. Thomas, *Proc. Natl. Acad. Sci. U.S.A.* **96**, 7394 (1999).
16. D. L. Riddle, Ed., *C. elegans II*, *Cold Spring Harbor Monogr. Ser.* **33** (Cold Spring Harbor Laboratory Press, Plainview, NY, 1997).
17. C. Trent, N. Tsuing, H. R. Horvitz, *Genetics* **104**, 619 (1983).
18. K. G. Miller *et al.*, *Proc. Natl. Acad. Sci. U.S.A.* **93**, 12593 (1996).
19. K. G. Miller, M. D. Emerson, J. B. Rand, *Neuron* **24**, 323 (1999).
20. D. A. Coulter, J. R. Huguenard, D. A. Prince, *Ann. Neurol.* **25**, 582 (1989).
21. J. C. Gomora, A. N. Daud, M. Weiergraber, E. Perez-Reyes, *Mol. Pharmacol.* **60**, 1121 (2001).
22. N. Leresche *et al.*, *J. Neurosci.* **18**, 4842 (1998).
23. Strains were provided by the *Caenorhabditis* Genetics Center, which is funded by the NIH National Center for Research Resources. We thank M. Nonet for helpful suggestions and *aex-3* mutants, S. Hughes for experimental assistance, and D. Redmond for assistance with graphics. Support was provided by the Washington University Alzheimer's Disease Research Center (grant no. P50 AG05681) and the Longer Life Foundation, a Reinsurance Group of

America, Inc. (RGA)/Washington University Partnership (grant no. 1999-001). C.H. was supported by a Predoctoral Fellowship from the Howard Hughes Medical Institute. K.K. is a scholar of the Leukemia and Lymphoma Society.

Supporting Online Material

www.sciencemag.org/cgi/content/full/307/5707/258/DC1

Materials and Methods

Fig. S1

References

16 September 2004; accepted 16 November 2004
10.1126/science.1105299

Self-Propagating, Molecular-Level Polymorphism in Alzheimer's β -Amyloid Fibrils

Aneta T. Petkova,¹ Richard D. Leapman,² Zhihong Guo,³ Wai-Ming Yau,¹ Mark P. Mattson,³ Robert Tycko^{1*}

Amyloid fibrils commonly exhibit multiple distinct morphologies in electron microscope and atomic force microscope images, often within a single image field. By using electron microscopy and solid-state nuclear magnetic resonance measurements on fibrils formed by the 40-residue β -amyloid peptide of Alzheimer's disease ($A\beta_{1-40}$), we show that different fibril morphologies have different underlying molecular structures, that the predominant structure can be controlled by subtle variations in fibril growth conditions, and that both morphology and molecular structure are self-propagating when fibrils grow from preformed seeds. Different $A\beta_{1-40}$ fibril morphologies also have significantly different toxicities in neuronal cell cultures. These results have implications for the mechanism of amyloid formation, the phenomenon of strains in prion diseases, the role of amyloid fibrils in amyloid diseases, and the development of amyloid-based nanomaterials.

Amyloid fibrils are self-assembled filamentous aggregates formed by peptides and proteins with diverse amino acid sequences (1). Current interest in amyloid fibrils arises from their involvement in Alzheimer's disease (AD), type 2 diabetes, prion diseases, and other protein misfolding disorders (2) and from basic questions about the interactions that stabilize amyloid structures and the mechanisms by which they form (3). Recent experiments additionally suggest that amyloid structures may be a basis for one-dimensional nanomaterials with possible technological applications (4, 5).

In transmission electron microscope (TEM) and atomic force microscope (AFM) images,

amyloid fibrils commonly exhibit multiple distinct morphologies, often described as twisted or parallel assemblies of finer protofilaments (6–8). Two explanations for amyloid polymorphism are possible: (i) distinct morphologies result from distinct modes of lateral association of protofilaments without significant variations in molecular structure (7) or (ii) distinct morphologies result from significant variations in molecular structure at the protofilament level. Here, we report electron microscopy and solid-state nuclear magnetic resonance (NMR) data on amyloid fibrils formed by the 40-residue β -amyloid peptide associated with AD ($A\beta_{1-40}$) that support the second possibility and reveal specific molecular-level structural differences between different fibril morphologies. The predominant morphology and molecular structure are sensitive to subtle differences in fibril growth conditions in de novo preparations (at fixed pH, temperature, buffer composition, and peptide concentration), but both morphology and molecular structure are self-propagating in seeded preparations. Different $A\beta_{1-40}$ fibril morphologies also exhibit significantly different toxicities in neuronal cell cultures.

¹Laboratory of Chemical Physics, National Institute of Diabetes and Digestive and Kidney Diseases, National Institutes of Health (NIH), Bethesda, MD 20892–0520, USA. ²Division of Bioengineering and Physical Science, Office of Research Services, NIH, Bethesda, MD 20892–5766, USA. ³Laboratory of Neurosciences, National Institute of Aging, NIH, Baltimore, MD 21224–6825, USA.

*To whom correspondence should be addressed.
E-mail: rt46d@nih.gov